Int. J. Heat Mass Transfer. Vol. 31, No. 5, pp. 993–1003, 1988
Printed in Great Britain

0017–9310/88 \$3.00+0.00

Thermal instability of two horizontal porous layers with a conductive partition

JIIN-YUH JANG and WEN-LIEH TSAI
Department of Mechanical Engineering, National Cheng-Kung University,
Tainan, Taiwan 70101, Republic of China

(*Received* 24 *June* 1987 *and in final form* 17 *September* 1987)

Abstract—The stability of two horizontal porous medium layers with a conductive partition is analysed by a linear stability theory. The upper cooled surface and the lower heated surface are taken to be isothermal and both are impermeable. The resulting eigenvalue problem is solved by a Galerkin method. The parameters affecting the stability limit are the ratio of two porous layer thicknesses, the ratio of partition thickness to total porous layer thickness, and the ratio of porous medium conductivity to partition thermal conductivity. Results show the system is most stable when the partition is located in the middle. In addition, as the partition thickness increases or the partition conductivity decreases, the system becomes more stable.

1. INTRODUCTION

NATURAL convection in a porous medium between two parallel plates with uniform heating from below is of interest to physicists, geophysicists and engineers. There are several important technical applications, for example, porous insulation development and geothermal energy conversion. A large number of theoretical and experimental studies on this subject has been made, see the review paper by Cheng [1]. The early work by Lapwood [2] determined the conditions for the onset of convection in a porous medium for a horizontal layer with isothermal boundaries and with impermeable and permeable upper surfaces. Critical Rayleigh numbers $Ra_{crit} = 4\pi^2$ (39.478) and 27.1 were obtained, respectively. The onset of natural convection in a porous layer under other boundary conditions has been discussed by Ribando and Torrance [3]. The critical Rayleigh numbers are 27.1 and 17.7 for a porous layer with a uniform heat flux from below and with impermeable and permeable upper surfaces, respectively. The effect of horizontal temperature gradients on the onset of free convection was investigated by Weber [4]. The analysis showed that the critical Rayleigh number is always higher than $4\pi^2$.

The convective heat transfer in fluid saturated porous beds either heated from below or heated by distributed sources was experimentally investigated by Buretta and Berman [5]. The critical Rayleigh numbers for the onset of convection are estimated as 38.0 for heating from below and 31.8 for distributed heat sources. The experiment by Close *et al.* [6] also confirmed $4\pi^2$ as the critical Rayleigh number.

This paper is concerned with the onset of natural convection in two horizontal porous medium layers with a conductive partition. The upper cooled surface and the lower heated surface are taken to be isothermal, and the fluid is governed by Darcy's law. This type of problem for the porous medium has not been studied in the literature. This has motivated the present investigation. It should be noted that the corresponding problem for a viscous fluid has been recently analysed by Catton and Lienhard [7]. The analysis of our paper is closely paralleled in ref. [7]; however, there are some differences, arising from the governing equations and the boundary condition on the velocity that differ in the two problems. As might be expected, the results for a porous medium resemble those for a viscous fluid. Linear stability theory is used and the resulting eigenvalue problem is solved by a Galerkin method. The effects of the thickness, location and thermal conductivity of the partition on the onset of convection of two porous layers are examined.

2. MATHEMATICAL ANALYSIS

Figure 1 represents the physical model and the coordinate system. By applying Darcy's law and the Boussinesq approximation, the governing equations for the physical model to be studied are

$$\frac{\partial u}{\partial x}+\frac{\partial v}{\partial y}=0 \quad (1)$$

$$\frac{\partial u}{\partial y}-\frac{\partial v}{\partial x}=-\frac{Kg\beta}{\nu}\frac{\partial T}{\partial x} \quad (2)$$

$$\sigma\frac{\partial T}{\partial t}+u\frac{\partial T}{\partial x}+v\frac{\partial T}{\partial y}=\alpha_e\left(\frac{\partial^2 T}{\partial x^2}+\frac{\partial^2 T}{\partial y^2}\right) \quad (3)$$

$$\rho=\rho_0[1-\beta(T-T_0)] \quad (4)$$

where σ is the heat capacity ratio of the saturated porous medium to that of the fluid, α_e the effective thermal diffusivity of the medium, K an empirical constant called permeability and β the fluid coefficient of volume expansion. Equations (1)–(4) must be satisfied in both porous layer regions.

NOMENCLATURE

A	ratio of partition thickness to total porous layer thicknesses, $L_p/(L_1+L_2)$
a	dimensionless disturbance wave number, $(2\pi/\lambda)L$
B	ratio of two porous layer thicknesses, L_2/L_1
g	gravitational acceleration
k_e	effective porous media thermal conductivity
k_p	partition thermal conductivity
K	permeability
L	thickness of layer
Ra	Darcy's Rayleigh number, defined in equations (15)
Ra_T	overall Rayleigh number, $Kg\beta(T_h-T_c)(L_1+L_p+L_2)/\alpha_e\nu$
T	temperature
T_c	temperature of the cold upper surface
T_h	temperature of the hot lower surface
u, v	Darcy's velocity in the x- and y-directions
V	dimensionless amplitude of the fluid velocity disturbance
x, y	Cartesian coordinates
Y	dimensionless y-coordinate.

Greek symbols

α_e	effective thermal diffusivity of the medium
β	fluid coefficient of volume expansion
θ	dimensionless amplitude of the temperature disturbance
λ	disturbance wavelength
ν	fluid kinematic viscosity
ρ	fluid density
σ	heat capacity ratio of the saturated porous medium to that of the fluid.

Subscripts

k	variable or parameter in porous region 1 or 2
p	partition
0	reference state quantity for the Boussinesq approximation.

Superscripts

$'$	disturbance quantity
*	dimensionless quantity
$-$	base state solution.

The horizontal velocity u can be eliminated by cross-differentiating between equations (1) and (2), leading to

$$\frac{\partial^2 v}{\partial x^2}+\frac{\partial^2 v}{\partial y^2}=\frac{Kg\beta}{\nu}\frac{\partial^2 T}{\partial x^2}. \tag{5}$$

In the partition we have

$$\frac{\partial T}{\partial t}=\alpha_p\left(\frac{\partial^2 T}{\partial x^2}+\frac{\partial^2 T}{\partial y^2}\right) \tag{6}$$

where α_p is the thermal diffusivity of the partition. The boundary conditions for these equations are

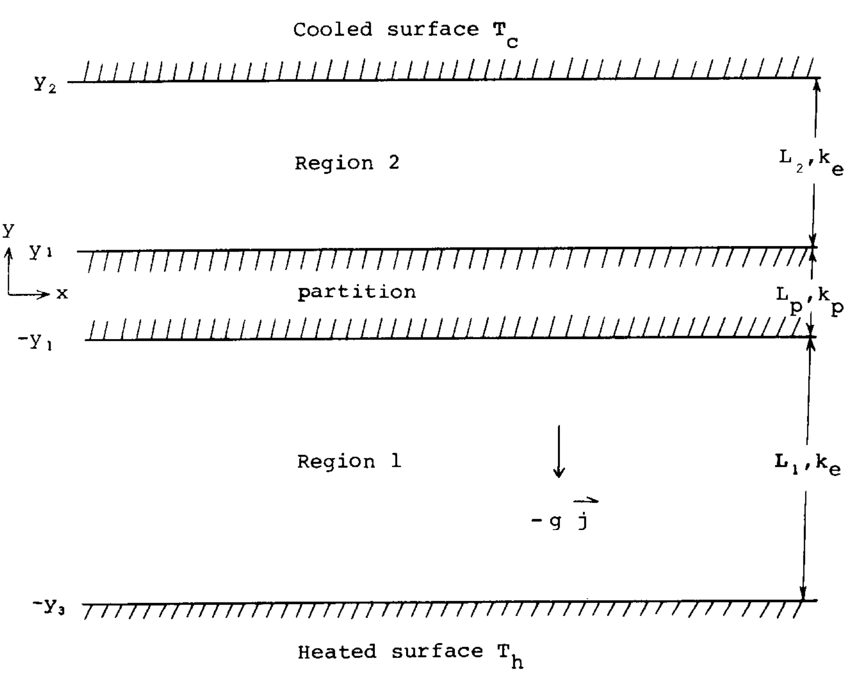

FIG. 1. The physical model and coordinate system.

$$v(x,-y_3) = v(x,-y_1) = v(x,y_1) = v(x,y_2) = 0$$
$$T(x,-y_3) = T_h, \quad T(x,y_2) = T_c \tag{7}$$

together with the matching of temperature and heat flux at the surfaces of the partition

$$y=-y_1, \quad T_1 = T_p, \quad -k_e\frac{\partial T_1}{\partial y} = -k_p\frac{\partial T_p}{\partial y} \tag{8}$$

$$y=y_1, \quad T_2 = T_p, \quad -k_e\frac{\partial T_2}{\partial y} = -k_p\frac{\partial T_p}{\partial y}. \tag{9}$$

The base state solutions for velocity and temperature are

$$\mathbf{V} = 0 \tag{10}$$

$$\bar{T}_1 = T_h - \frac{T_h - T_c}{\left(1+\frac{L_2}{L_1}+\frac{L_p}{k_p}\frac{k_e}{L_1}\right)}\left(\frac{y+y_3}{L_1}\right),$$
$$-y_3 \leqslant y \leqslant -y_1 \tag{11}$$

$$\bar{T}_p = T_h - \frac{T_h - T_c}{\left(1+\frac{L_2}{L_1}+\frac{L_p}{k_p}\frac{k_e}{L_1}\right)}\left(1+\frac{k_e}{L_1}\frac{L_p}{k_p}\frac{(y+y_1)}{L_p}\right),$$
$$-y_1 \leqslant y \leqslant y_1 \tag{12}$$

$$\bar{T}_2 = T_h - \frac{T_h - T_c}{\left(1+\frac{L_2}{L_1}+\frac{L_p}{k_p}\frac{k_e}{L_1}\right)} \times \left(1+\frac{k_e}{L_1}\frac{L_p}{K_p}+\frac{L_2}{L_1}\frac{(y-y_1)}{L_2}\right),$$
$$y_1 \leqslant y \leqslant y_2. \tag{13}$$

To perform a linear stability analysis, we first perturb the base state solutions and write

$$T(x,y,t) = \bar{T}(y) + T'(x,y,t)$$
$$v(x,y,t) = 0 + v'(x,y,t). \tag{14}$$

On introducing the following transformations:

$$t_k^* = \frac{t}{L_k^2\sigma/\alpha_e}, \quad v_k^* = \frac{v_k'}{\alpha_e/L_k}, \quad y_k^* = \frac{y}{L_k},$$
$$y_p^* = \frac{y}{L_p}, \quad x_k^* = \frac{x}{L_k}, \quad x_p = \frac{x}{L_p},$$
$$t_p^* = \frac{t}{L_p^2/\alpha_p}, \quad T_k^* = \frac{T_k'}{\Delta T_k},$$
$$T_p^* = \frac{T_p'}{\Delta T_1}, \quad Ra_k = \frac{Kg\beta\Delta T_k L_k}{\alpha_e \nu} \tag{15}$$

note that $k = 1,2$ where ΔT_k is the temperature difference across porous region k, $k = 1,2$ and Ra_k is the individual Darcy's Rayleigh number. Then equations (2)–(6) are linearized, using standard procedures for the stability analysis. Thus, we find

$$\frac{\partial T_k^*}{\partial t_k^*} - v_k^* = \frac{\partial^2 T_k^*}{\partial x_k^{*2}} + \frac{\partial^2 T_k^*}{\partial y_k^{*2}} \tag{16}$$

$$\frac{\partial^2 v_k^*}{\partial x_k^{*2}} + \frac{\partial^2 v_k^*}{\partial y_k^{*2}} = Ra_k\frac{\partial^2 T_k^*}{\partial x_k^{*2}} \tag{17}$$

$$\frac{\partial^2 T_p^*}{\partial x_p^{*2}} + \frac{\partial^2 T_p^*}{\partial y_p^{*2}} = \frac{\partial T_p^*}{\partial y_p^*}. \tag{18}$$

Assuming solutions to equations (16)–(18) are of the form

$$v_k^* = V_k(Y_k)e^{(s_k t_k^* + ia_k x_k^*)}$$
$$T_k^* = \theta_k(Y_k)e^{(s_k t_k^* + ia_k x_k^*)}$$
$$T_p^* = \theta_p(Y_p)e^{(s_p t_p^* + ia_p x_p^*)} \tag{19}$$

where a is the wave number of the disturbance in the x-direction, s the growth rate, and V and θ amplitudes of disturbances in the vertical velocity component and the temperature profiles, respectively. Substituting equations (19) into equations (16)–(18) and setting $s = 0$ for neutral stability, we have:

for region 1

$$(D_1^2 - a_1^2)V_1 = -a_1^2 Ra_1\theta_1 \tag{20}$$
$$(D_1^2 - a_1^2)\theta_1 = -V_1 \tag{21}$$
$$Y_1 = y_1^* + \frac{y_3}{L_1} - \tfrac{1}{2} \quad \text{and} \quad -\tfrac{1}{2} \leqslant Y_1 \leqslant \tfrac{1}{2};$$

for region 2

$$(D_2^2 - a_2^2)V_2 = -a_2^2 Ra_2\theta_2 \tag{22}$$
$$(D_2^2 - a_2^2)\theta_2 = -V_2 \tag{23}$$
$$Y_2 = y_2^* - \frac{y_1}{L_2} - \tfrac{1}{2} \quad \text{and} \quad -\tfrac{1}{2} \leqslant Y_2 \leqslant \tfrac{1}{2};$$

for the partition

$$(D_p^2 - a_p^2)\theta_p = 0 \tag{24}$$
$$Y_p = \frac{y}{L_p} \quad \text{and} \quad -\tfrac{1}{2} \leqslant Y_p \leqslant \tfrac{1}{2}$$

where D_k denotes d/dY_k, $k = 1, 2, p$.

The wave numbers are all related to a common disturbance wavelength

$$a_1 = 2\pi L_1/\lambda, \quad a_2 = 2\pi L_2/\lambda, \quad a_p = 2\pi L_p/\lambda. \tag{25}$$

The boundary conditions for equations (20)–(24) are

$$V_k(\pm\tfrac{1}{2}) = \theta_1(-\tfrac{1}{2}) = \theta_2(\tfrac{1}{2}) = 0, \quad k = 1,2$$

and

$$\theta_1(\tfrac{1}{2}) = \theta_p(-\tfrac{1}{2}), \quad B\theta_2(-\tfrac{1}{2}) = \theta_p(\tfrac{1}{2})$$
$$A(1+B)\frac{k_e}{k_p}D_1\theta_1(\tfrac{1}{2}) = D_p\theta_p(-\tfrac{1}{2})$$
$$A(1+B)\frac{k_e}{k_p}D_2\theta_2(-\tfrac{1}{2}) = D_p\theta_p(\tfrac{1}{2}) \tag{26}$$

where $A = L_p/(L_1+L_2)$ is the ratio of the partition thickness to the total porous layer thickness and $B = L_2/L_1$ is the ratio of two porous layer thicknesses.

Equations (20)–(24) with equations (26) form an eigenvalue problem for Ra_1 and Ra_2 with A, B and k_e/k_p as parameters.

3. NUMERICAL METHOD

The method of solution is that of Galerkin as described in Catton and Lienhard [7]. First, V_k ($k = 1,2$) are expanded in terms of orthogonal functions which satisfy the boundary conditions on V_k. We assume the velocities have the form

$$V_k = \sum_i A_i^k \psi_i^k(Y_k), \quad k = 1,2 \tag{27}$$

where

$$\psi_i^k(Y_k) = \begin{cases} \cos(i\pi Y), & i = 1,3,5\ldots \\ \sin(i\pi Y), & i = 2,4,6\ldots \end{cases} \tag{28}$$

The corresponding temperature profiles θ_k can be obtained by substituting equation (27) into equations (21) and (23)

$$\theta_k = \sum_i A_i^k \phi_i^k(Y_k) + D^k \cosh(a_k Y_k) + E^k \sinh(a_k Y_k) \tag{29}$$

where

$$\phi_i^k = \begin{cases} \dfrac{1}{(i\pi)^2 + a_k^2}\cos(i\pi Y_k), & i = 1,3,5\ldots \\ \dfrac{1}{(i\pi)^2 + a_k^2}\sin(i\pi Y_k), & i = 2,4,6\ldots \end{cases} \tag{30}$$

The disturbance temperature θ_p in the partition is obtained directly from equation (24)

$$\theta_p = M\cosh(a_p Y_p) + N\sinh(a_p Y_p). \tag{31}$$

The constants M, N, D^k and E^k are found by satisfying the boundary conditions on θ at the heated and cooled surfaces, and the matching conditions at the partition. The result is given as

$$\theta_k(Y_k) = \sum_i A_i^k \Phi_i^{kk}(Y_k) + \sum_i A_i^j \Phi_i^{kj}(Y_k)$$

note that

$$\begin{cases} j = 2 & \text{as } k = 1 \\ j = 1 & \text{as } k = 2 \end{cases} \tag{32}$$

where Φ_i^{kk} and Φ_i^{kj} are the same as those given in Catton and Lienhard [7]. The derivations are quite lengthy and are omitted here. The details are given in Tsai [8].

Substituting the derived expression for θ_k and the assumed series for V_k into equations (20) and (22) and then weighting and integrating over the regions ($k = 1,2$) yielding the following matrix equation:

$$\left(\begin{array}{c|c} \bar{\bar{L}} + a_1^2 Ra_1 \bar{\bar{N}} & a_1^2 Ra_1 \bar{\bar{I}} \\ \hline a_2^2 Ra_2 \bar{\bar{J}} & \bar{\bar{M}} + a_2^2 Ra_2 \bar{\bar{K}} \end{array}\right) \cdot \left(\begin{array}{c} A^1 \\ \hline A^2 \end{array}\right) = 0 \tag{33}$$

where

$$\bar{\bar{L}} = \int_{-1/2}^{1/2} \psi_j^1(D_1^2 - a_1^2)\psi_i^1 \, dY_1,$$

Table 1. The critical Rayleigh number of region 1, Ra_1, for different integration interval points n with $B = 1.0$, $k_e/k_p = 1.0$ and $N = 6$

A	n = 11	21	31	41	51
0.01	27.4017	27.4036	27.4037	27.4037	27.4037
0.1	29.2496	29.2479	29.2479	29.2479	29.2479
0.3	31.5995	31.5914	31.5914	31.5914	31.5914
1.0	32.9077	32.9015	32.9014	32.9015	32.9015

$$\bar{\bar{J}} = \int_{-1/2}^{1/2} \psi_j^2 \Phi_i^{21} \, dY_2,$$

$$\bar{\bar{N}} = \int_{-1/2}^{1/2} \psi_j^1 \Phi_i^{11} \, dY_1,$$

$$\bar{\bar{M}} = \int_{-1/2}^{1/2} \psi_j^2(D_2^2 - a_2^2)\psi_i^2 \, dY_2,$$

$$\bar{\bar{I}} = \int_{-1/2}^{1/2} \psi_j^1 \Phi_i^{12} \, dY_1,$$

$$\bar{\bar{K}} = \int_{-1/2}^{1/2} \psi_j^2 \Phi_i^{22} \, dY_2. \tag{34}$$

Noting that $Ra_2 = B^2 Ra_1$ and $a_2^2 = B^2 a_1^2$ and applying the requirement for non-trivial solutions, i.e. the determinant of the first matrix of equation (33) is zero, we obtain

$$\left| \left(\begin{array}{c|c} \bar{\bar{L}} & \bar{\bar{O}} \\ \hline \bar{\bar{O}} & \bar{\bar{M}} \end{array}\right) + a_1^2 Ra_1 \left(\begin{array}{c|c} \bar{\bar{N}} & \bar{\bar{I}} \\ \hline B^4 \bar{\bar{J}} & B^4 \bar{\bar{K}} \end{array}\right) \right| = 0. \tag{35}$$

This has the form of a generalized eigenvalue problem, and, for a specified a_1, Ra_1 is the eigenvalue. The choice of an N-term approximation for velocity yields a $2N \times 2N$ matrix, the minimum eigenvalue of which is the desired Rayleigh number. To find the critical Rayleigh number for given values of A, B and k_e/k_p, first, the values of Ra_1 are calculated for several selected values of a_1, and then a curve fitting is established through these points, and finally letting $dRa_1/da_1 = 0$ to find the critical Rayleigh number.

To check the numerical accuracy, we compute some cases for different shape function terms N and interval points n when equations (34) are integrated using Simpson's 3/8 rule. The results for the critical Rayleigh number of region 1, Ra_1, are presented in Tables 1 and 2. It is seen that the results are accurate to at least three significant digits when a six-term shape function is used in conjunction with 21 point Simpson's 3/8 rule of the integral.

4. DISCUSSION OF RESULTS

The critical Rayleigh numbers Ra_1, Ra_2 and Ra_T are presented in Table 3 for $0.01 \leqslant A \leqslant 1.0$, $0.125 \leqslant B \leqslant 1.0$, and $0 \leqslant k_e/k_p \leqslant 100$, where

Table 2. The critical Rayleigh number of region 1, Ra_1, for different shape function terms N with $B = 1.0$, $k_e/k_p = 1.0$ and $n = 21$

A	n = 4	6	8
0.01	27.4081	27.4036	27.4031
0.1	29.2483	29.2479	29.2477
0.3	31.5923	31.5914	31.5910
1.0	32.9122	32.9015	32.9011

$$Ra_T = Kg\beta(T_h - T_c)(L_1 + L_p + L_2)/\alpha_e \nu$$

is the overall critical Rayleigh number. The critical Rayleigh number of either layer is related to Ra_1 by

$$Ra_T = Ra_1(1+B)^2(1+A)(1+A(k_e/k_p))$$

and

$$Ra_2 = Ra_1 B^2.$$

Results are given only for $B \leqslant 1$ because of the principle of symmetry. Calculations were also performed for $B = 2$, 4 and 8, and the results were in good agreement with those for $B = 0.5$, 0.25 and 0.125. This confirms the principle of symmetry.

In Table 3, $k_e/k_p = 0$ corresponds to the case when the partition is a perfect conductor, i.e. isothermal, and there is no temperature gradient in it. This reduces to the classical Bénard problem for a porous medium. The computed Ra_1 is 39.477 as compared to the exact value of $4\pi^2$ (39.478) as obtained in ref. [2]. When $k_e/k_p \to \infty$, as indicated by Catton and Lienhard [7] for a viscous fluid, the boundary condition at the partition approaches that for a constant heat flux. We calculated Ra_1 for $k_e/k_p = 10^5$, 10^6, 10^7 with $A = 1.0$ and $B = 1.0$ and obtained $Ra_1 = 27.1654$, 27.1652, 27.1651, respectively, which are in good agreement with the value of 27.16 as obtained in ref. [3]. These comparisons also confirm the accuracy of our numerical computation.

Figures 2(a)–(d) show the variation of Ra_T as a function of conductivity ratio k_e/k_p for $A = 0.01$, 0.1, 0.3 and 1.0, respectively, and for various values of B. It is seen that, for a given k_e/k_p, the porous layer is most stable when the partition is located in the middle. The rapid drop in Ra_T as k_e/k_p increases from zero, results from decreasing damping of the thermal disturbance in the partition. This drop is smoother for larger values of A, since a thicker partition provides more damping for the disturbance. This trend is also observed for a viscous fluid [7]. As k_e/k_p increases, for a given B, the system becomes more stable because the thermal conductivity of the partition decreases, which in turn decreases the temperature gradient over each porous layer (for a fixed value of $T_h - T_c$).

Figures 3(a)–(d) illustrate the variation of Ra_T as a function of the conductivity ratio k_e/k_p for $B = 0.125$, 0.25, 0.5 and 1.0, respectively, for selected values of A. It is shown that, for a given conductivity ratio, the system becomes more stable as the ratio of the

Table 3. The critical Rayleigh numbers Ra_1, Ra_2 and Ra_T

	$B = 0.125$			$B = 0.25$			$B = 0.5$			$B = 1.0$		
k_e/k_p	Ra_1	Ra_2	Ra_T	Ra_1	Ra_2	Ra_T	Ra_1	Ra_2	Ra_T	Ra_1	Ra_2	Ra_T
						$A = 0.01$						
0.0	39.48	0.62	50.47	39.48	2.47	62.30	39.48	9.87	89.73	39.48	39.48	159.51
0.2	36.22	0.57	46.39	34.84	2.18	55.10	33.38	8.35	76.01	28.29	28.29	114.53
1.0	35.94	0.56	46.40	34.47	2.15	54.94	32.83	8.21	75.34	27.40	27.40	111.82
5.0	35.16	0.55	47.19	33.84	2.12	56.08	32.31	8.08	77.09	27.21	27.21	115.44
10.0	34.38	0.53	48.35	33.24	2.08	57.70	31.85	7.96	79.63	27.19	27.19	120.83
100.0	29.76	0.47	76.10	29.45	1.84	92.95	29.04	7.26	132.00	27.17	27.17	219.51
						$A = 0.1$						
0.0	39.48	0.62	54.96	39.48	2.47	67.86	39.48	9.87	97.72	39.48	39.48	173.72
0.2	36.78	0.57	52.24	36.27	2.27	63.60	36.07	9.02	91.05	33.78	33.78	151.60
1.0	34.72	0.54	53.18	33.84	2.12	63.98	32.87	8.22	89.51	29.24	29.24	141.50
5.0	31.25	0.49	65.26	30.76	1.92	79.30	30.19	7.55	112.07	27.62	27.62	182.34
10.0	29.83	0.47	83.07	29.53	1.85	101.53	29.16	7.29	144.32	27.40	27.40	241.12
100.0	27.54	0.43	421.79	27.51	1.72	520.04	27.45	6.86	747.40	27.19	27.19	1315.96
						$A = 0.3$						
0.0	39.48	0.62	64.94	39.48	2.47	80.20	39.48	9.87	115.48	39.48	39.48	205.31
0.2	37.21	0.58	64.89	37.14	2.32	79.97	37.17	9.29	115.26	36.64	36.64	201.99
1.0	33.57	0.52	71.80	33.12	2.07	87.45	32.91	8.23	125.16	31.59	31.59	213.58
5.0	29.52	0.46	121.41	29.36	1.84	149.12	29.19	7.30	213.44	28.32	28.32	368.22
10.0	28.50	0.45	187.57	28.41	1.78	230.85	28.30	7.08	331.13	27.77	27.77	577.55
100.0	27.32	0.43	1393.37	27.31	1.71	1719.58	27.29	6.82	2474.93	27.23	27.23	4389.12
						$A = 1.0$						
0.0	39.48	0.62	99.94	39.48	2.47	123.38	39.48	9.87	177.67	39.48	39.48	315.87
0.2	37.35	0.58	113.44	37.35	2.33	140.05	37.35	9.34	201.67	37.34	37.34	358.44
1.0	32.93	0.51	166.72	32.93	2.06	205.80	32.93	8.23	296.35	32.90	32.90	526.46
5.0	28.96	0.45	439.88	28.96	1.81	542.96	28.96	7.24	781.75	28.93	28.93	1388.58
10.0	28.13	0.44	783.22	28.13	1.76	966.82	28.13	7.03	1392.07	28.11	28.11	2473.37
100.0	27.27	0.42	6971.36	27.27	1.70	8606.47	27.27	6.82	12 393.22	27.27	27.27	22 030.59

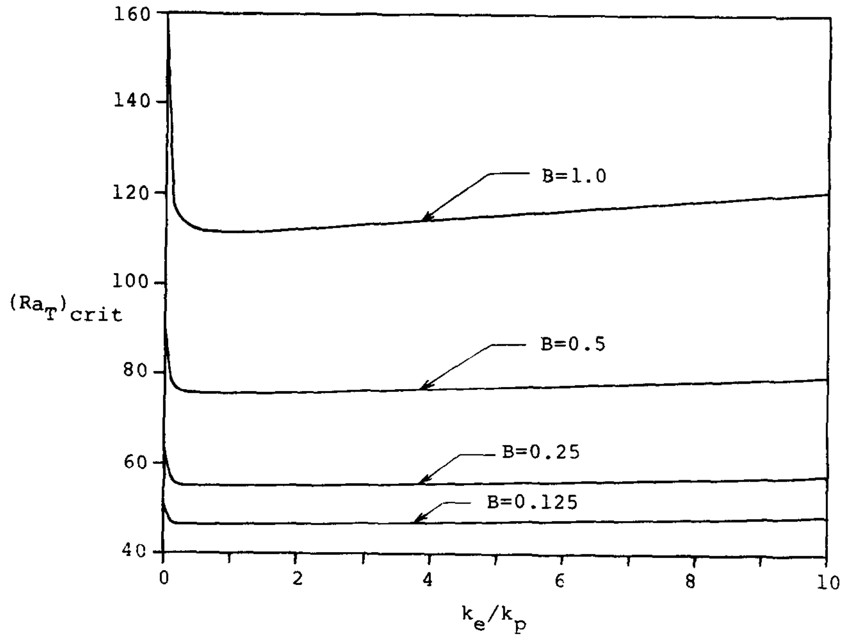

FIG. 2(a). The effect of partition location and conductivity upon the stability of the porous layers for $A = 0.01$.

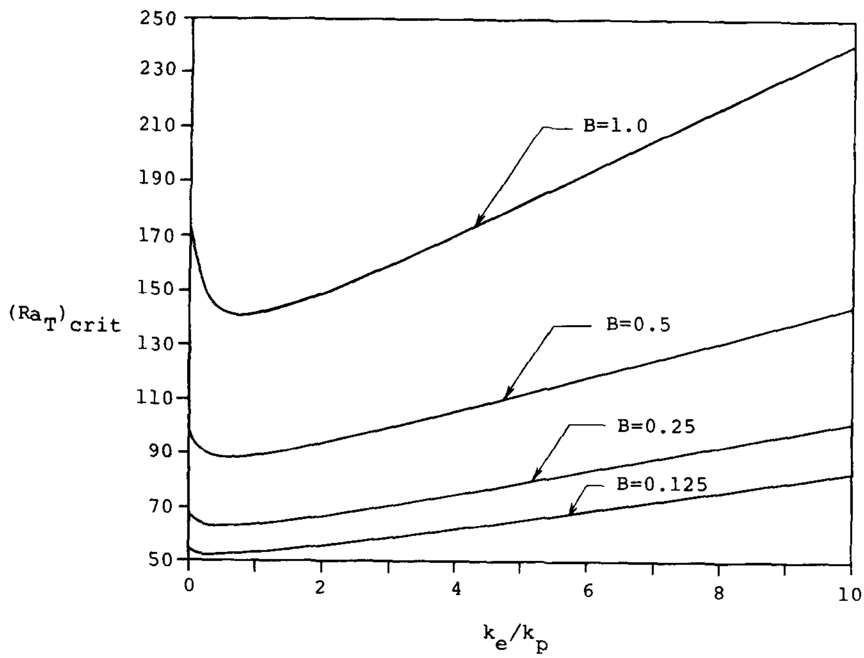

FIG. 2(b). The effect of partition location and conductivity upon the stability of the porous layers for $A = 0.1$.

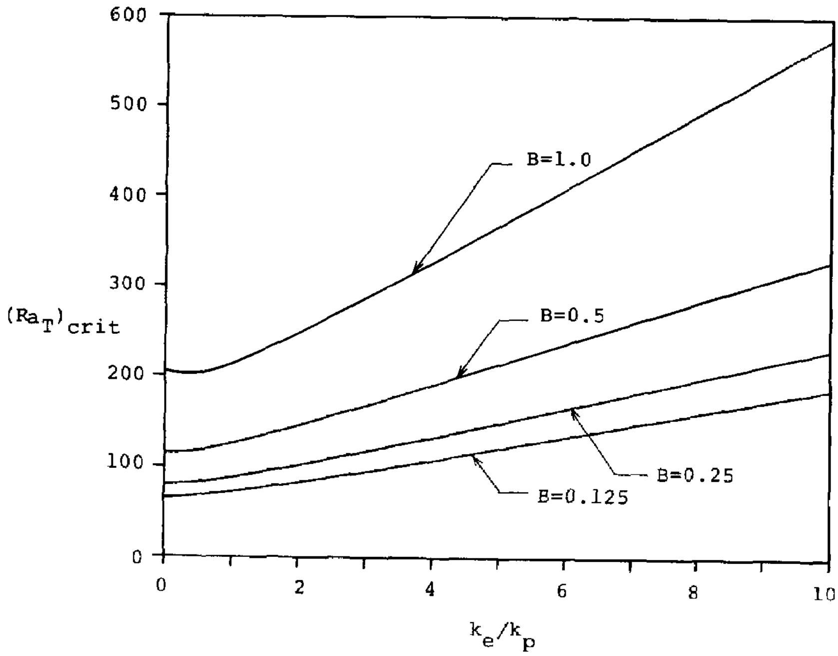

FIG. 2(c). The effect of partition location and conductivity upon the stability of the porous layers for $A = 0.3$.

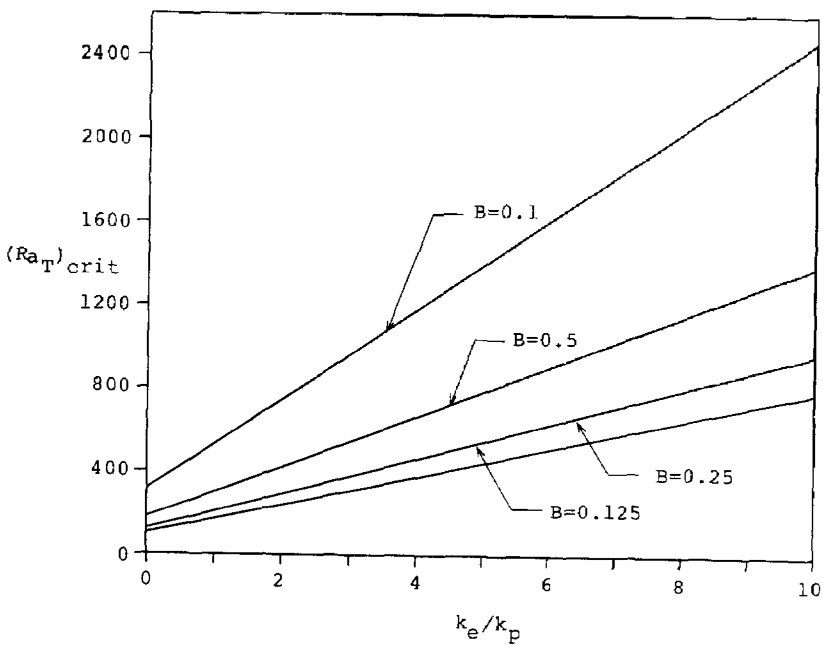

FIG. 2(d). The effect of partition location and conductivity upon the stability of the porous layers for $A = 1.0$.

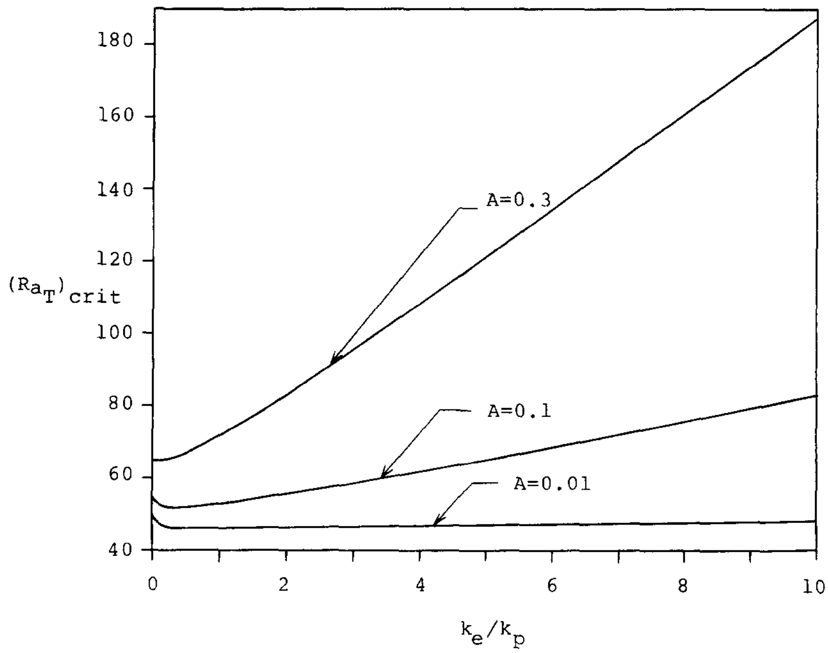

FIG. 3(a). The effect of partition thickness and conductivity upon the stability of the porous layers for $B = 0.125$.

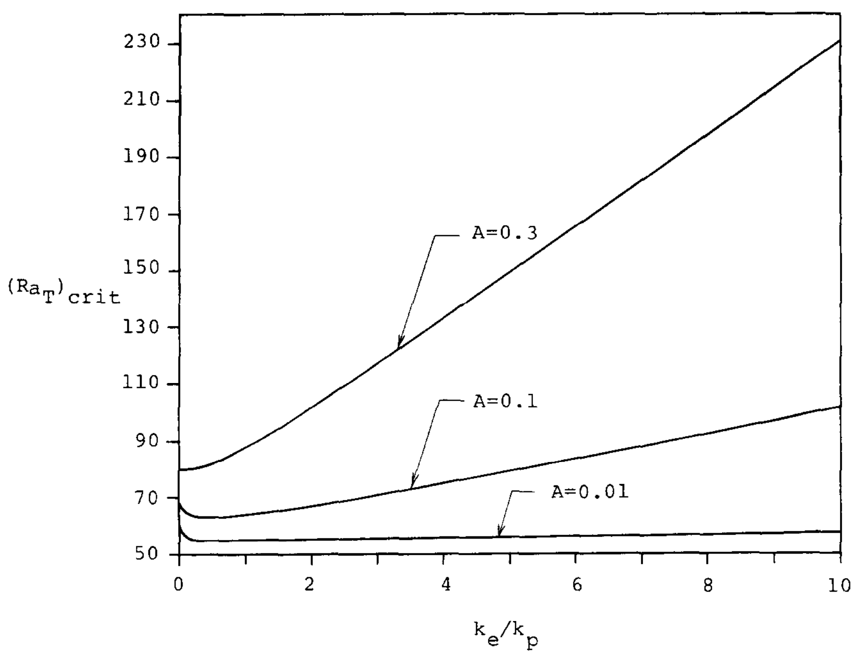

FIG. 3(b). The effect of partition thickness and conductivity upon the stability of the porous layers for $B = 0.25$.

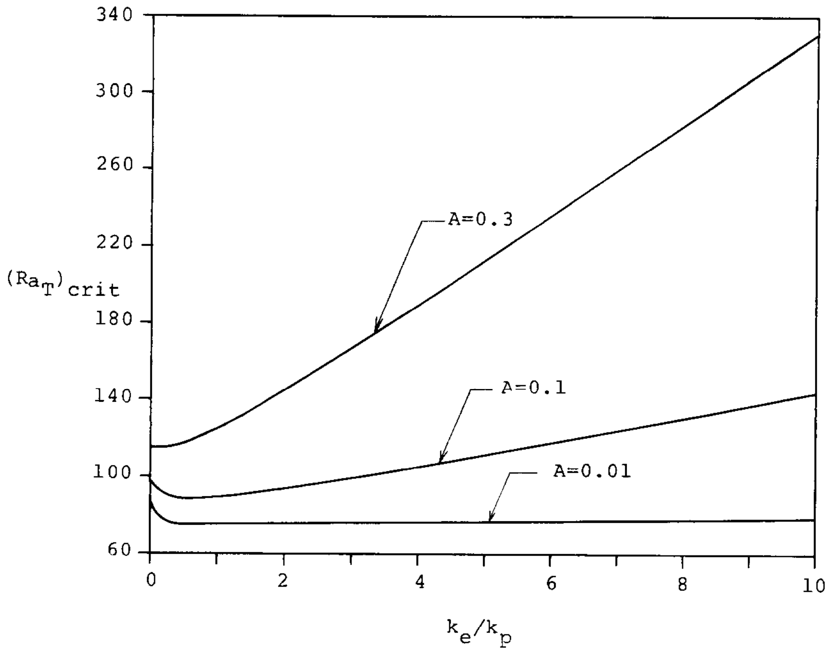

FIG. 3(c). The effect of partition thickness and conductivity upon the stability of the porous layers for $B = 0.5$.

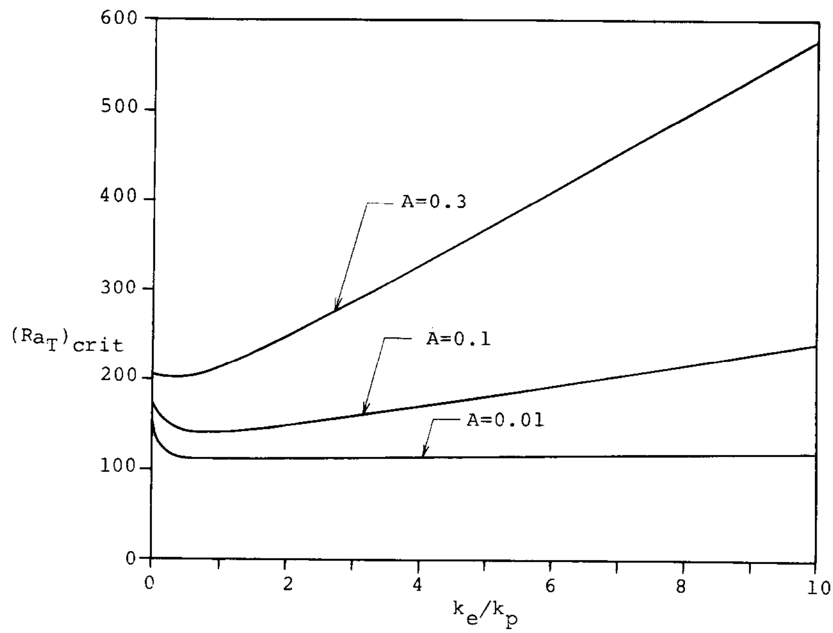

FIG. 3(d). The effect of partition thickness and conductivity upon the stability of the porous layers for $B = 1.0$.

partition thickness to total porous layer thickness, A, increases. As indicated before, this is due to the fact that a thicker partition can greatly damp the disturbances. It is also seen that, for $A = 0.01$, i.e. thinner partition, the overall stability is not significantly affected by the partition conductivity. However, the overall stability is profoundly dependent on the partition location as seen in Fig. 2(a).

5. CONCLUSION

The stability of the onset of thermal convection of two horizontal porous medium layers with a conductive partition has been investigated using the linear stability theory. The qualitative results are similar to those for a viscous flow in the absence of a porous medium. It is shown that the system is most stable when the partition is located in the middle. In addition, the system is much more stable than that without partition even though the partition is quite thin. For example, for $A = 0.01$, $B = 1.0$ and $k_e/k_p = 1$, the overall critical Rayleigh number is 111.82, which is much larger than $4\pi^2$ for a system without partition. Results also indicate that as the partition thickness increases or the partition conductivity decreases, the system becomes more stable. The results presented in this paper provide useful information for the analysis of insulating layers.

REFERENCES

1. P. Cheng, Heat transfer in geothermal system, *Adv. Heat Transfer* **14**, 1–100 (1978).
2. E. R. Lapwood, Convection of a fluid in a porous medium, *Proc. Camb. Phil. Soc.* **44**, 508–521 (1948).
3. R. J. Ribando and K. E. Torrance, Natural convection in a porous medium: effect of confinement, variable permeability, and thermal boundary conditions, *ASME J. Heat Transfer* **95**, 42–48 (1976).
4. J. E. Weber, Convection in a porous medium with horizontal and vertical temperature gradients, *Int. J. Heat Mass Transfer* **17**, 241–248 (1974).
5. R. J. Buretta and A. S. Berman, Convective heat transfer in a liquid saturated porous layer, *ASME J. Appl. Mech.* 248–253 (1976).
6. D. J. Close, J. G. Symons and R. F. White, Convective heat transfer in shallow, gas-filled porous media: experimental investigation, *Int. J. Heat Mass Transfer* **28**, 2371–2378 (1985).
7. I. Catton and J. H. V. Lienhard, Thermal stability of two fluid layer separated by a solid interlayer of finite thickness and thermal conductivity, *ASME J. Heat Transfer* **106**, 605–612 (1984).
8. W. L. Tsai, Thermal instability of two horizontal porous layers with a conductive partition, Master's thesis, Department of Mechanical Engineering, National Cheng-Kung University, Tainan, Taiwan (1987).

INSTABILITE THERMIQUE DE DEUX COUCHES POREUSES HORIZONTALES AVEC UNE PARTITION CONDUCTIVE

Résumé—La stabilité de deux couches poreuses horizontales avec une partition conductive est analysée par une théorie linéaire de stabilité. La surface supérieure froide et la surface inférieure chaude sont isothermes et imperméables. Le problème de valeurs propres est résolu par une méthode de Galerkin. Les paramètres agissant sur la limite de stabilité sont le rapport des épaisseurs des deux couches, le rapport de l'épaisseur de partition à l'épaisseur totale poreuse et le rapport de la conductivité du milieu poreux à celle de la partition thermique. Les résultats montrent que le système est plus stable quand la partition est située au milieu. En outre, lorsque l'épaisseur de partition augmente ou lorsque la conductivité de partition décroît, le système devient plus stable.

THERMISCHE INSTABILITÄT ZWEIER HORIZONTALER PORÖSER SCHICHTEN MIT WÄRMELEITENDER KONTAKTZONE

Zusammenfassung—Es wird die Stabilität zweier horizontaler poröser Stoffschichten mit wärmeleitender Kontaktzone durch ein lineares Stabilitätsverfahren untersucht. Die gekühlte obere Fläche und die beheizte untere Oberfläche werden als Isothermenflächen angenommen, wobei beide Flächen stoffundurchlässig sind. Das resultierende Eigenwertproblem wird durch ein Galerkin-Verfahren gelöst. Die Stabilitätsgrenze wird durch die folgenden Parameter beeinflußt: das Verhältnis zweier poröser Schichtdicken, das Verhältnis von Kontaktschichtdicke zu gesamter poröser Schichtdicke und das Verhältnis der Wärmeleitfähigkeiten von porösem Medium und Kontaktschicht. Es wird gezeigt, daß bei mittiger Lage der Kontaktzone die besten Systemstabilitäten zu erwarten sind. Zusätzlich wird das System mit zunehmender Kontaktschichtdicke oder abnehmender Wärmeleitfähigkeit der Kontaktzone stabiler.

ТЕПЛОВАЯ НЕУСТОЙЧИВОСТЬ ДВУХ ГОРИЗОНТАЛЬНЫХ ПОРИСТЫХ СЛОЕВ С ПРОВОДЯЩЕЙ ПЕРЕГОРОДКОЙ

Аннотация—С помощью теории линейной устойчивости анализируется устойчивость двух горизонтальных пористых слоев с проводящей перегородкой. Верхняя охлаждаемая и нижняя нагреваемая поверхности полагаются изотермическими и непроницаемыми. Полученная задача на собственные значения решается методом Галеркина. Параметрами, влияющими на предел устойчивости, являются отношение толщин пористых слоев, отношение толщины перегородки к суммарной толщине пористого слоя и отношение теплопроводностей пористой среды и перегородки. Результаты покаывают, что система наиболее устойчива в случае, когда перегородка расположена в центре. Кроме того, при увеличении толщины перегородки или уменвшении ее проводимости система становится более устойчивой.